

Published in final edited form as:

Vision Res. 2011 January 28; 51(2): 251–259. doi:10.1016/j.visres.2010.10.016.

Overlapping spatiotemporal patterns of regulatory gene expression are required for neuronal progenitors to specify retinal ganglion cell fate

Takae Kiyama^a, Chai-An Mao^a, Jang-Hyeon Cho^a, Xueyao Fu^a, Ping Pan^a, Xiuqian Mu^{a,*}, and William H. Klein^{a,b,†}

^aDepartment of Biochemistry and Molecular Biology, The University of Texas MD Anderson Cancer Center, Houston, Texas USA

^bGraduate Training Program in Genes and Development, The University of Texas Graduate School of Biomedical Sciences, Houston, Texas

Abstract

Retinal progenitor cells (RPCs) are programmed early in development to acquire the competence for specifying the seven retinal cell types. Acquiring competence is a complex spatiotemporal process that is still only vaguely understood. Here, our objective was to more fully understand the mechanisms by which RPCs become competent for specifying a retinal ganglion cell (RGC) fate. RGCs are the first retinal cell type to differentiate and their abnormal development leads to apoptosis and optic nerve degeneration. Previous work demonstrated that the paired domain factor Pax6 and the bHLH factor Atoh7 are required for RPCs to specify RGCs. RGC commitment is marked by the expression of the Pou domain factor Pou4f2 and the Lim domain factor Isl1. We show that three RPC subpopulations can specify RGCs: *Atoh7*-expressing RPCs, *Neurod1*-expressing RPCs, and *Atoh7-Neurod1*-expressing RPCs. All three RPC subpopulations were highly interspersed throughout retinal development, although each subpopulation maintained a distinct temporal pattern. Most, but not all, RPCs from each subpopulation were postmitotic. *Atoh7-Neurod1* double knockout mice were generated and double mutant retinas revealed an unexpected role for Neurod1 in specifying RGC fate. We conclude that RPCs have a complex regulatory gene expression program in which they acquire competence using highly integrated mechanisms.

Keywords

Retinal development; retinal progenitor cells; retinal ganglion cells; cell cycle; homeobox factor Pax6; proneural bHLH factors Atoh7; Neurod1

© 2010 Elsevier Ltd. All rights reserved.

[†]Corresponding author. Address: Department of Biochemistry and Molecular Biology, The University of Texas MD Anderson Cancer Center, Houston, TX 77030, USA whklein@mdanderson.org.

^{*}Present address: Department of Ophthalmology/Ross Eye Institute, Center of Excellence in Bioinformatics and Life Sciences, University of Buffalo, Buffalo, NY 14203 USA

Publisher's Disclaimer: This is a PDF file of an unedited manuscript that has been accepted for publication. As a service to our customers we are providing this early version of the manuscript. The manuscript will undergo copyediting, typesetting, and review of the resulting proof before it is published in its final citable form. Please note that during the production process errors may be discovered which could affect the content, and all legal disclaimers that apply to the journal pertain.

1. Introduction

In the past twenty years, an impressive amount of knowledge has been generated on molecular regulatory mechanisms that control retinal development in embryonic and neonatal life (for a recent review, see Agathocleous and Harris, 2009). Many of these mechanisms have been found to be important in the preservation of the adult retina as well (Lamba and Reh, 2008). Despite this substantial knowledge database, we still remain woefully uninformed about many of the fundamental mechanisms that are required to generate a fully functional neural tissue capable of receiving light and sending the information to the visual centers in the brain for visual perception.

Retinal development begins immediately after the presumptive retinal epithelial layer separates from the presumptive retinal pigmented epithelium and retinal progenitor cells (RPCs) arise from pluripotent neural stem cells. RPCs are intrinsically programmed at very early stages in retinal development to follow certain lineage paths but they are not yet committed to any of the seven retinal cell types (Livesey and Cepko, 2001, Agathocleous and Harris, 2009). Rather, RPCs become competent over developmental time to commit to one or more individual cell types. RPC competency changes continuously during retinogenesis as the extrinsic environment of the developing retina changes (Livesey and Cepko, 2001, Agathocleous and Harris, 2009). RPC competency is marked by the expression of transcriptional regulatory factors. Expression of the paired box-homeodomain factor *Pax6* is necessary for the specification of all the retinal cell types except amacrine cells (Marquardt et al., 2001; Marquardt and Gruss, 2002; Oron-Karni et al., 2008). *Pax6* action is counteracted by the Notch-Delta signaling pathway, which keeps RPCs in the cell cycle by activating the bHLH transcriptional repressors *Hes1* and *Hes5* (Agathocleous and Harris, 2009; Riesenberger et al., 2009b).

In this present study, we focus on the development of one of the seven retinal cell types, retinal ganglion cells (RGCs). In the mouse, as with other vertebrates, RGCs are the first cells to differentiate from RPCs. For RGC commitment to occur, a population of *Pax6*-expressing RPCs must downregulate the Notch signaling pathway, exit the cell cycle, and express the proneural bHLH gene *Atoh7* (also called *Math5*) (Mu and Klein, 2004, 2008; Agathocleous and Harris, 2009). These events render *Pax6-Atoh7*-RPCs competent for specifying the RGC lineage.

Lineage analysis has shown that in addition to RGCs, *Atoh7*-expressing RPCs can give rise to all the other retinal cell types (Yang et al., 2003). Indeed, most *Atoh7*-expressing cells are thought not to form RGCs (T. Glaser, unpublished results). However, retinas of *Atoh7*-knockout mice lack virtually all RGCs yet still form all the other retinal cell types (Brown et al, 2001; Wang et al., 2001). *Atoh7* is therefore necessary but not sufficient for commitment to an RGC fate (Yang et al., 2003; Mu and Klein, 2008). In the mouse retina, the earliest signs of overt RGC differentiation are the downregulation of *Atoh7* expression and the onset of expression of two key transcription factors that are essential for normal RGC differentiation to occur. These are the Pou domain factor *Pou4f2* and the Lim domain factor *Isl1* (Gan et al., 1999; Mu et al., 2008; Pan et al., 2008). *Pou4f2*, *Isl1*, and most likely other early-expressing transcriptional regulators activate a hierarchical RGC gene regulatory network consisting of more downstream transcription factors as well as secreted signaling molecules that feedback to RPCs to maintain a correct balance of proliferating RPCs and differentiating RGCs (Mao et al., 2008a; Mu and Klein, 2008; Mu et al., 2008).

To fully understand how RPCs give rise to RGCs, more precise analyses are required than those that have been previously reported. Towards this end, we recently generated a mouse line in which *Atoh7* is replaced with a hemagglutinin (HA) epitope-tagged knock-in

construct (*Atoh7-HA*) (Fu et al., 2009). Retinal cells expressing *Atoh7-HA* can be readily recognized by immunohistochemical methods using an anti-HA antibody. The *Atoh7-HA-knock-in mice* provide the means to examine over spatiotemporal development the relationship of *Atoh7*-expressing RPCs with other transcriptional regulators and with markers of cell cycle progression. Our results show that distinct populations of *Atoh7*-expressing RPCs are present in the developing retina and reveal an unexpected role for the proneural bHLH gene *Neurod1* in specifying a subpopulation of RGCs. We conclude that RPCs are far more heterogeneous than previously thought and that they exhibit a complex regulatory gene expression program in which they acquire competence using highly integrated mechanisms.

2. Methods

2.1. Genetically engineered mice

Atoh7-knockout mice are described in Wang et al. (200), *Neurod1*-knockout mice are described in Pennesi et al. (2003), and *Atoh7-HA* mice are described in Fu et al. (2009). *Atoh7-Neurod1*-double heterozygous and double homozygous mice were generated by breeding single mutant heterozygous and homozygous mice. Mice were genotyped by Southern blot analysis or PCR using tail DNA as previously described (Fu et al., 2009). Embryos were designated embryonic day (E) 0.5 at noon on the day in which vaginal plugs were observed.

All animal procedures in this study follow the United States Public Health Service Policy on Humane Care and Use of Laboratory Animals and were approved by the Institutional Animal Care and Use Committee at The University of Texas MD Anderson Cancer Center.

2.2. Immunohistochemical analysis and X-gal staining

Embryos or eyes were collected and fixed with 4% paraformaldehyde for 30 min, washed three times with PBST (PBS pH7.4, 0.2% Tween 20), embedded in OCT and frozen. Sixteen-micron cryosections were collected, washed 3 times for 10 min with PBST, and blocked with 2% BSA in PBST for 1 hr. For some staining, frozen or paraffin-embedded sections were placed in a microwave oven at 600 W in 10 mM sodium citrate for 18 min to expose the antigen epitopes, and then blocked in 10% normal serum and 0.1% Tween 20 for 1 hr at room temperature. The sections were then incubated with primary antibodies with appropriate dilution in 2% BSA-PBST for 1 hr. X-gal staining was done as described elsewhere (Mao et al., 2008a). Primary antibodies were anti-HA (Santa Cruz, 1:800), anti-Pax6 (DSHB, 1:400), anti-Chx10 (Exalpha, 1:300, Covance, 1:1000), anti-NeuroD (Santa Cruz Biotechnology, 1:400), anti-cyclinD1 (Cell Signaling, 1:300), anti-lacZ (Cell Signaling, 1:400), anti-Chat (Swant, 1:500), anti-calbindin (Swant, 1:500), anti-glutamate synthase (Sigma, 1:300), anti-rhodopsin (Cell Sigma, 1:500), anti-NFL (InVitrogen, 1:200), anti-B-opsin and anti-R-opsin (1:500, Chemicon). Secondary antibodies were conjugates of Alexa Fluor 488 and Alexa Fluor 555 (InVitrogen). Secondary antibodies were conjugates of Alexa Fluor 488 and Alexa Fluor 555 (Invitrogen). DAPI (4', 6-diamidino-2-phenylindole) or PI (propidium iodide) were used as a nuclear counterstain. Sections were washed with PBST and mounted in Fluoromount G (EMS) and examined under a confocal microscope.

2.3. BrdU labeling

For BrdU labeling, 0.1 mg of BrdU per g body weight was injected intraperitoneally into pregnant mice one hour prior to euthanization. Embryos were fixed and washed for immunohistochemistry, embedded in OCT and frozen. Sixteen-micron of cryosection were washed three times with PBST for 10 min followed by 4N HCl treatment for 1 hr. Sections

were washed three times with PBST for 10 min and incubated with anti-BrdU antibody (Upstate, 1:5). Alexa 488-conjugated anti-mouse IgG antibody was used for secondary antibody labeling.

2.4. Retina flat-mount analysis

To detect RGC axons, eyes were removed from postnatal mice and fixed with 4% paraformaldehyde for 30 min. The cornea, ciliary band, and lens were removed using a pair of iris scissors. The remaining retinal tissue and attached pigmented epithelium were fixed for 1 hr and then washed four times in PBS saline and 0.1% Triton X-100 at room temperature. The retinas were then incubated in blocking solution (PBST plus 5% fetal bovine serum) for 1 hr, and incubated with anti-NFL (1:250) for 48 hr at 4°C. Retinas were washed four times with PBST and stained with Alexa488-conjugated goat anti-mouse IgG1 secondary antibody (Invitrogen). After washing thoroughly with PBS, the pigmented epithelium was removed from the retinas and four or five symmetrical cuts were made halfway from the peripheral rim to the central optic disk. Retinas were then flat-mounted onto glass slides and analyzed using an Olympus FluoView1000 confocal microscope.

2.5. Determination of cell number

Cell number was determined by cell counting as described previously (Mu *et al.*, 2005). Sections from three individual retinas were used for each staining. Two confocal images of central retinal region from each section were taken and cells stained in the neuroblast layer were counted. The neuroblast layer was determined based on morphology. Number of HA-expressing cells was represented as a fraction of cells stained with HA antibody per cells stained with PI. For co-immunostaining, numbers of cells were represented as fractions of cells stained by HA and Pax6, Chx10 or NeuroD1 antibodies per cells stained by HA antibody.

3. Results

3.1. Characterization of Atoh7-HA expression with an anti-HA antibody

Because a robust anti-Atoh7 antibody for immunohistochemistry is not available, we recently generated and characterized *Atoh7-HA* knock-in mice, which could then be used to detect *Atoh7*-expression with any number of well-described, commercially available anti-HA antibodies (Fu *et al.*, 2009). To determine whether immunohistochemical labeling with anti-HA antibody accurately reflected endogenous *Atoh7* expression in developing retinas, we made use of *Atoh7-lacZ* knock-in mice that had been previously generated in our laboratory (Wang *et al.* 2001). E14.5 retinas from *Atoh7^{lacZHA}* heterozygous mice were immunohistochemically labeled with anti-HA antibody and histologically stained for X-gal (Fig. 1A). HA-positive cells were detected in the neuroblast layer but not in the ganglion cell layer, whereas lacZ-stained cells were present in both the neuroblast and ganglion cell layers (Fig. 1A). In the neuroblast layer, approximately 65% of the HA-labeled cells were also labeled with lacZ. However, 35% of the HA-positive cells were not co-labeled with lacZ, and similarly, we observed lacZ-positive cells that were not labeled with HA (Fig. 1A). HA-positive cells were found distributed throughout the neuroblast layer, while lacZ-positive cells accumulated more in the ventricular region than the central region of the neuroblast layer. Because lacZ is known to be a highly stable protein, the differences observed between HA-positive cells and lacZ-positive cells might reflect differences in the stabilities of lacZ and Atoh7-HA proteins. The stability of the Atoh7-HA fusion protein was likely to be more similar to that of Atoh7, which is thought to have a higher turnover rate than lacZ (Wang *et al.*, 2001; Fu *et al.*, 2009). If this was the case, Atoh7-HA labeling would be indicative of cells expressing *Atoh7* in a narrower time window than those expressing lacZ, whose expression might reflect the more long-term history of cells that once expressed *Atoh7* but

were no longer doing so. Despite this caveat, the majority of cells in the neuroblast layer of E14.5 retinas were co-labeled with HA and lacZ, supporting the view that the anti-HA antibody was a suitable proxy for *Atoh7*-expressing cells.

Atoh7-HA mice provide a means to determine many of the features of *Atoh7*-expressing RPCs that have been difficult to determine by other methods. For example, neither the time when *Atoh7* exerts its activity or the fraction of *Atoh7*-expressing RPCs in the neuroblast layer of the developing retina has been accurately determined. If *Atoh7-HA* expression does in fact accurately reflect *Atoh7*-expression, it is reasonable to assume that all the rates associated with the synthesis, processing, and degradation of *Atoh7-HA* mRNA and protein are the same as the corresponding rates for *Atoh7* mRNA and protein. To obtain a clearer picture of the temporal expression pattern of *Atoh7* and number of *Atoh7*-expressing RPCs, we immunolabeled retinas at different developmental times with anti-HA antibody. In E12.5 retinas, approximately 20% of cells in the neuroblast layer were HA positive (Fig. 1B). The fraction of cells expressing *Atoh7-HA* increased until E14.5, when 27% of the cells in the neuroblast layer were expressing *Atoh7-HA*. The fraction of HA-positive cells then rapidly declined; only 8% of the cells were HA positive at E17.5, and only 2% were positive at E19.5 (Fig. 1B). HA-positive cells were not detected in adult retinas (date not shown). These results were consistent with and considerably extend those reported previously (Brown et al., 1998; Wang et al., 2001; Willardsen et al., 2009).

3.2. *Atoh7*- HA-expression in proliferating RPCs

Two previously published reports differed on when in the cell cycle RPCs are expressing *Atoh7*. One study using *Atoh7-Cre* and *Rosa26-lacZ* expression to determine the lineage of *Atoh7*-expressing RPCs found that all *Atoh7*-expressing RPCs were postmitotic (Yang et al., 2003). However, a second study using an *Atoh7-lacZ* knock-in line and antibodies against the cell cycle kinase inhibitor p27/Kip1 found that *Atoh7* was expressed in cells exiting the cell cycle, and in fact was required for cell cycle exit to occur normally (Le et al., 2006). In an attempt to resolve these differences and determine more directly whether *Atoh7* was expressed in proliferating RPCs, we co-labeled developing retinas with anti-HA and anti-Chx10 antibodies. Chx10 is a homeobox transcription factor that is required for RPC proliferation and for bipolar cell development (Burmeister et al., 1996; Hatakeyama et al., 2001; Dyer, 2003; Liang and Sandell, 2008). From E12.5 to E19.5, Chx10-positive cells were observed uniformly distributed throughout the neuroblast layer (Fig. 2A–2D). During these times, HA-positive cells were detected both in Chx10-positive and Chx10-negative cells (Fig. 2A–2D). The fraction of HA-positive cells co-expressing *Chx10* ranged from 20–30% from E12.5 until E18.5, and declined to 8% at E19.5 (Fig. 3). In contrast to the earlier studies of Yang et al. (2003) and Le et al. (2006), our results indicated that many *Atoh7*-expressing RPCs were actively proliferating. The reason for the discrepancies in the three studies is not clear. Our approach was to use anti-HA and anti-Chx10 antibody co-labeling, which was clearly distinct from the approaches used in the other studies. It is possible that HA labeling overestimates the number of *Atoh7*-expressing RPCs that are in the cell cycle while the other approaches underestimate this value.

To confirm our results with Chx10, we used other cell cycle indicators in conjunction with anti-HA antibody labeling. BrdU was used to determine the number of *Atoh7*-expressing RPCs that were in the S-phase of the cell cycle. Cells positive for both HA and BrdU and cells positive for HA but not BrdU were observed in the neuroblast layer (Fig. 4A). Approximately 25% of the HA-positive cells were co-labeled with anti-BrdU antibody. We observed a similar labeling pattern using anti-cyclinD1 antibody, which marks the G-phase of the cell cycle (Fig. 4B). Approximately 25% of the HA-positive cells were co-labeled with anti-cyclinD1. We also used an anti-p27 antibody (Fig. 4C). In this case, approximately half of the HA-positive cells were also labeled with anti-p27 antibody. These results differ

substantially from those observed by Lee et al. (2003) using an anti-p27 antibody and lacZ expression. In contrast to Yang et al. (2003) and Lee et al. (2006), our experiments suggested that although the majority of *Atoh7*-expressing RPCs in the developing retina were postmitotic, many were also in RPCs that were actively dividing.

3.3. Co-expression of *Atoh7* with *Pax6*

Pax6 and *Atoh7* are essential for RGC development, yet the relationship between these two critical transcription factors during retinal development is only vaguely understood. A recent report describes a cis-regulatory element upstream of *Atoh7* whose activity depends on *Pax6*, suggesting that *Atoh7* is a direct *Pax6* target gene (Riesenberg et al., 2009a). To further address this issue, we determined the extent to which *Pax6* and *Atoh7* were co-expressed during retinal development by co-labeling retinas at different developmental times with anti-*Pax6* and anti-HA antibodies. At E12.5, almost 90% of the cells in the neuroblast layer of the retina that were expressing *Atoh7*-HA were also expressing *Pax6* (Fig. 3; Fig. 5A). The fraction of *Atoh7*-HA-expressing cells that were also expressing *Pax6* decreased to 78% at E13.5, and by E14.5, this fraction had decreased to 45% and continued to steadily decline to 42%, 30%, and 23% by E15.5, E16.5, and E17.5, respectively (Fig. 3; Fig. 5A–5C). At E18.5 and E19.5, no co-labeling was observed (Fig. 3; Fig. 5D). These results reinforced the view that during the critical times when RPCs are acquiring competence to specify an RGC fate, the expression of both *Pax6* and *Atoh7* is required.

3.4. Co-expression of *Atoh7* with *Neurod1*

Neurod1 is a proneural bHLH factor that shares significant sequence similarity to *Atoh7* (Vetter and Brown, 2001; Mao et al. 2008b). In retinal development, *Neurod1* has been shown to be necessary for amacrine cell formation and for the maintenance of rod photoreceptor cells (Inoue et al., 2002; Pennesi et al., 2003). Using a gene knock-in construct designed for gene replacement at the *Atoh7* locus, we recently demonstrated that *Neurod1* could partially replace the functions of *Atoh7* when it is expressed at the same time and place as *Atoh7* (Mao et al., 2008b). One interpretation of our results was that *Neurod1* played some role in RGC development in addition to its other roles in amacrine cell development and rod photoreceptor maintenance. We hypothesized that the functions for *Atoh7* and *Neurod1* as well as for other proneural bHLH factors expressed during retinogenesis were far more synergistic and integrated than what had previously been suggested (Mao et al., 2008b).

To gain further insight into the possible interactions between *Atoh7* and *Neurod1*, we co-labeled developing retinas with anti-HA and anti-*Neurod1* antibodies. At E12.5, we detected HA-positive cells and *Neurod1*-positive cells distributed throughout the neuroblast layer (Fig. 5E). By E14.5, *Neurod1*-positive cells were largely restricted to the outer nuclear layer and this pattern was maintained as development proceeded (Fig. 5G–5H). Throughout development, we found that 20–30% of HA-positive cells were also *Neurod1*-positive (Fig. 3; Fig. 5E–5H). The results indicated that a significant population of *Atoh7*-expressing RPCs was also expressing *Neurod1*, and provided further support to the notion that *Neurod1* played a role in RGC development.

3.5. Generation and characterization of *Atoh7*-*Neurod1* double knockout mice

Despite the importance of *Atoh7* in specifying RGC fate, a small fraction of seemingly normal RGCs persist in *Atoh7*-null retinas (Lin et al., 2004; Moshiri et al., 2008). These experiments, together with our recent results showing that *Neurod1* could replace *Atoh7*, suggested the possibility of an *Atoh7*-independent program that required *Neurod1* to generate a small subpopulation of RGCs. To determine whether this was the case, we generated *Atoh7*-*Neurod1* double knockout mice and compared their retinas with *Atoh7*-null

retinas. Adult retinas from *Atoh7-Neurod1* double knockout mice maintained their laminar integrity but overall were very thin when compared with *Atoh7*-null or wild-type retinas (Fig. 6). Overall retinal thinness is often a sign of decreased RPC proliferation or increased apoptosis during retinal development.

To determine whether any of the retinal cell types were affected in the double-mutant retinas, we immunohistochemically labeled adult retinas with a number of antibodies that labeled specific retinal cell types, namely, anti-Chat (amacrine cells, Fig. 6A–6C), anti-M-opsin (M-cone photoreceptors, Fig. 6A–6C), anti-NFL (RGCs, Fig. 6D–6F), anti-S-opsin (S-cone photoreceptors, Fig. 6D–6F), anti-glutamine synthase (GS) (Müller glial cells, Fig. 6G–6I), anti-rhodopsin, (rod photoreceptors, Fig. 6J–6L), Chx10 (bipolar cells, Fig. 6M–6O), and anti-calbindin (horizontal cells, Fig. 6M–6O).

We detected a significant decrease in the number of M-cone photoreceptors in double mutant retinas (none detectable) compared with *Atoh7*-null (65.33 ± 6.11) or wild-type retinas (91.67 ± 4.04) (Fig. 6A–6C). The loss of M-cone photoreceptors in *Neurod1*-knockout mice has recently been found to be associated with an overproliferation of S-cone photoreceptors at the expense of M-cone photoreceptors, yet we did not detect a difference in the number of M-cone cells between the *Neurod1*^{-/-} and double mutants (Liu et al., 2008). Other additional defects were also seen in *Atoh7-Neurod1* double mutant retinas; e.g. calbindin-positive amacrine cells were decreased in the inner nuclear layer of double mutant retinas (217 ± 25.53) compared to that in control retinas (272 ± 7.55). These data suggested that *Atoh7* does not compensate for *Neurod1* in cone cell formation. In addition, the perinuclear condensation of rhodopsin that we observed in the rod photoreceptors of the double mutants (Fig. 6L) was a sign of rod photoreceptor degeneration, which has been previously reported in *Neurod1*-null retinas by Pennesi et al. (2003).

Importantly, we also observed a significant decrease in NFL expression in *Atoh7-Neurod1* double mutant retinas compared with *Atoh7*-null retinas (Fig. 6E, 6F). Although NFL expression was strongly downregulated in *Atoh7*-null retinas compared with wild-type controls (Fig. 6D, 6E), the diminishment of NFL expression was even more pronounced in the double mutant retinas (Fig. 6F). These results indicated that the loss of RGCs was even greater in *Atoh7-Neurod1* double mutant retinas than in *Atoh7*-null retinas. This was particularly interesting because RGCs develop normally in *Neurod1*-null mice (Pennesi et al., 2003).

We determined the number of RGCs in double mutant retinas more directly using flat-mounted retina preparations that were immunolabeled with anti-NFL antibody to detect RGC axons (Fig. 7A–7D). We detected significantly fewer RGC axons in double mutant retinas than in *Atoh7*-null retinas (compare Fig. 7A, 7C with Fig. 7B, 7D). To determine whether the enhanced RGC phenotype is due to a specification or a maintenance defect, we immunostained E13.5 retinal sections with an anti-Pou4f2 antibody. We found that the remaining few Pou4f2-positive cells in the *Atoh7* mutant were completely abolished in the *Atoh7-Neurod1* double mutant (Fig. 8B, C). Furthermore, we conducted apoptosis analysis on mutant retinas, and found a slight increase of dying cells in the *Atoh7-Neurod1* double mutant compared to that of the control (Fig. 9). The results were consistent with our hypothesis that *Neurod1* contributed to RGC development and that it was required for the formation of a subpopulation of RGCs that formed in the absence of *Atoh7*.

4. Discussion

The ability to generate mouse models using targeted gene knockout technology has resulted in major advances in our understanding of the mechanisms that regulate retinal development

(e.g., Chalupa and Williams, 2008). In the present study, we made use of two genetically engineered mouse lines, one that expressed an *Atoh7*-HA allele at the *Atoh7* locus and another that lacked both the *Atoh7* and *Neurod1* genes. The experiments described in this report relied on these mouse lines to provide new insights into RPCs and how they acquire the competency for specifying the retinal cell types. The results lead to the conclusion that RPCs are far more complicated in their expression of regulatory genes than previously thought. Furthermore, regulatory genes expressed in RPCs are likely to be synergistic and to operate in complex combinations to advance a competent RPC to a committed retinal cell type.

Immunolabeling with anti-HA antibody allowed us to determine the spatiotemporal expression pattern of *Atoh7* and the fraction of RPCs that express *Atoh7* during retinal development. We found that *Atoh7* was expressed in a narrow window of time, with expression peaking at E14.5 and rapidly declining thereafter. At E12.5, the earliest time we examined, *Atoh7*-expressing RPCs already represented 20% of the cells in the neuroblast layer, and at its peak, *Atoh7* was expressed in more than one-quarter of the cells. Thus, *Atoh7* must be activated at very early times in retinal development and *Atoh7*-expressing RPCs must make a significant contribution to the initial but not final stages of retinogenesis. This is particularly interesting because most *Atoh7*-expressing RPCs are not destined to follow an RGC fate (Yang et al., 2003). Earlier reports have shown that *Atoh7* has additional functions besides those for RGC fate specification, which are not easily revealed by knockout and other loss-of-function approaches (Brown et al., 2001, Wang et al., 2001, Le et al., 2006). We favor a model in which *Atoh7*-expressing RPCs play critical roles in broader aspects of retinal cell type specification, especially at early times in retinogenesis. *Atoh7* is likely to work together with *Pax6* and other transcription factors in defining one subpopulation of RPCs during these times.

An unexpected finding from our experiments was that in addition to postmitotic RPCs, a fraction of proliferating RPCs also express *Atoh7*. Although our results appear to contradict previous studies (Yang et al., 2003; Le et al., 2006), they are consistent with a model in which proliferating RPCs activate *Atoh7* expression and that this activation is closely coupled to cell cycle exit. The time in the cell cycle when *Atoh7* is expressed may be highly sensitive to the method of detection. Because a robust antibody for *Atoh7* is not available and in situ hybridization is limited by the abundance of *Atoh7* transcripts and technical difficulty in double labeling with cell cycle markers, less direct methods are required. Nevertheless, all experiments reported to date are consistent with a model in which the majority of *Atoh7*-expressing RPCs are just exiting or have exited the cell cycle.

Pax6 plays a broader role in retinal development than *Atoh7* (Marquardt and Gruss, 2002) and is positioned genetically upstream of *Atoh7* in a model for a RGC gene regulatory network that we have proposed (Mu and Klein, 2008; Mu et al., 2008). The *Pax6*-HA co-labeling experiments further support the view *Pax6* and *Atoh7* must be co-expressed in the same RPC in order for it to acquire competency for an RGC fate. It is also likely that co-expression of *Pax6* and *Atoh7* is important for the formation of other retinal cell types, although this remains to be shown.

Kageyama and co-workers have proposed that retinal cell-fate specification is regulated by combinations of bHLH and homeobox genes. In their model, homeobox genes confer positional identity whereas bHLH genes promote neuronal cell fate specification (Hatakeyama et al., 2001; Hatakeyama and Kageyama, 2004; Ohsawa and Kageyama, 2008). Some bHLH factors are known to function as transcriptional activators (e.g., *Atoh7*, *Neurod1*) and others as transcriptional repressors (e.g., *Hes1*, *Hes5*). In addition, bHLH factors regulate each other's expression (Mu et al., 2005; Le et al., 2006; Ohsawa and

Kageyama, 2008). In RPCs of the developing retina, these interactions occur in dynamic spatiotemporal patterns. It is therefore likely that an exceedingly complicated transcriptional network regulates retinal development.

Earlier work suggested that *Neurod1*-expressing and *Atoh7*-expressing RPCs are largely distinct populations with differing spatiotemporal expression patterns (Inoue et al., 2002; Mu et al., 2005). Our results indicate that there is a substantial number of RPCs that co-express *Neurod1* and *Atoh7*. Thus, three distinct subpopulations of RPCs co-exist during the early stages of retinal development, *Atoh7*-expressing RPCs, *Neurod1*-expressing RPCs, and *Atoh7-Neurod1*-expressing RPCs.

We showed previously that a *Neurod1* knock-in construct inserted at the *Atoh7* locus resulted in partial, but not full, activation of the RGC gene regulatory network and restoration of RGCs and the optic nerve (Mao et al., 2008b). The close relatedness of *Neurod1* and *Atoh7* sequences in their bHLH domains indicates that these transcription factors may have extensive overlap in the gene regulatory networks that they activate. However, *Neurod1* is thought to play different roles in retinal cell-fate specification than those played by *Atoh7*. *Neurod1* and a related bHLH gene, *Math3*, are required together for amacrine cell-fate specification (Inoue et al., 2002). The fact that many RPCs co-express *Neurod1* and *Atoh7*, and that fewer RGCs are present in *Atoh7-Neurod1* double knockout retinas compared with *Atoh7* single knockout retinas, strongly argues that *Neurod1* plays a role in RGC development. *Neurod1* may synergize with *Atoh7* to promote RGC specification, and in addition, *Neurod1* may be required for the development of a subpopulation of RGCs that form independently of *Atoh7*.

Recently, we demonstrated a role for the neuronal transcriptional repressor REST/NRSF in retinal development (Mao et al., 2010). REST/NRSF is an engrailed domain-containing transcriptional repressor that represses the expression of neuronal differentiation genes in non-neuronal cells, pluripotent stem cells, and neuronal progenitors (Kagalwala et al., 2008). Six3-Cre-mediated deletion of a floxed *REST/NRSF* allele leads to the efficient deletion of *REST/NRSF* in the developing retina beginning at E10.5 (Mao et al., 2010). We found that in the absence of *REST/NRSF*, many of the genes that are normally expressed in differentiated RGCs are prematurely activated in proliferating RPCs (Mao et al., 2010). Most importantly, the premature expression of RGC genes was independent of *Atoh7*, as shown by the expression of some of the genes in RPCs of *Atoh7-REST/NRSF* double knockout retinas. These results led to the hypothesis that a distinct pathway for formation of a subpopulation of RGCs exists in the developing retina. This pathway is suppressed by *REST/NRSF* and does not depend on the presence of *Atoh7*. From the results presented here, we suggest that *Neurod1* is required for the *Atoh7*-independent pathway to operate.

In summary, our results provide further demonstration of the complexity of the gene regulatory networks that are required for retinal development. Emerging new technologies using next generation genomic and cDNA sequencing offer a potentially valuable way to identify the downstream components of retinal gene regulatory networks. A more detailed picture of these networks and the crucial nodes within them should eventually lead to a more comprehensive understanding of the molecular programs that regulate retinal cell-fate specification and to how these programs are altered by the continuously changing extrinsic environment of the developing retina.

Acknowledgments

We thank Ming-Jer Tsai (Baylor College of Medicine) for providing the *Neurod1* mice. We acknowledge The University of Texas MD Anderson Cancer Center DNA Analysis Facility for DNA sequencing, the Genetically Engineered Mouse Facility and the Research Animal Support Facility for providing their services. The Core

Facilities are supported in part by a National Cancer Institute Cancer Center Core Grant (CA016672). The work was supported by grants to W.H.K. from the National Eye Institute (EY011930 and EY010608-139005) and from the Robert A. Welch Foundation (G-0010).

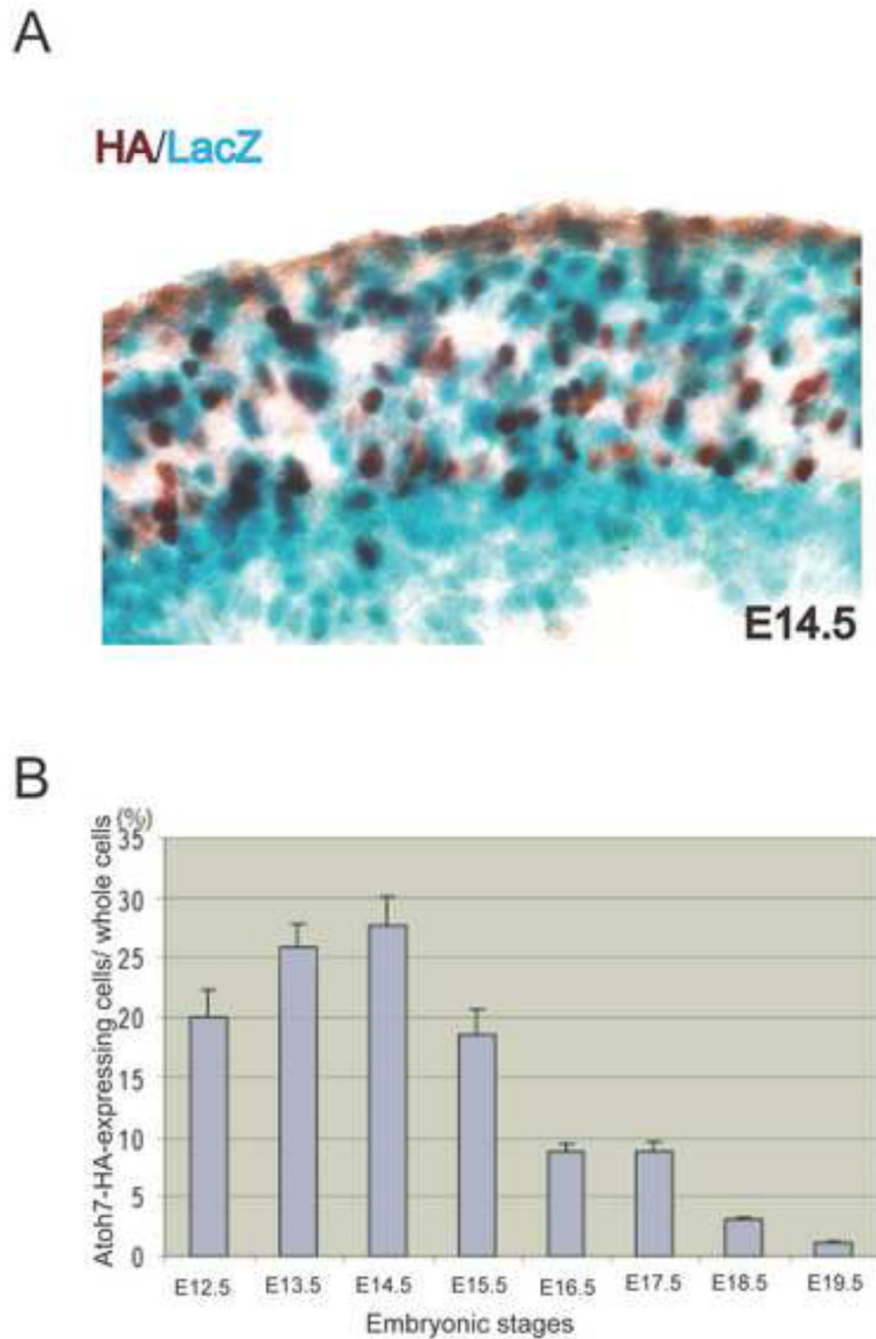
References

- Agathocleous M, Harris WA. From progenitors to differentiated cells in the vertebrate retina. *Annu. Rev. Cell Dev. Biol.* 2009; 25:45–69. [PubMed: 19575661]
- Brown NL, Kanekar S, Vetter ML, Tucker PK, Gemza DL, Glaser T. Math5 encodes a murine basic helix-loop-helix transcription factor expressed during early stages of retinal neurogenesis. *Development.* 1998; 125:4821–4833. [PubMed: 9806930]
- Brown NL, Patel S, Brzezinski J, Glaser T. Math5 is required for retinal ganglion cell and optic nerve formation. *Development.* 2001; 128:2497–2508. [PubMed: 11493566]
- Burmeister M, Novak J, Liang MY, Basu S, Ploder L, Hawes NL, Vidgen D, Hoover F, Goldman D, Kalnins VI, Roderick TH, Taylor BA, Hankin MH, McInnes RR. Ocular retardation mouse caused by Chx10 homeobox-null allele: impaired retinal progenitor proliferation and bipolar cell differentiation. *Nat. Genet.* 1996; 12:376–384. [PubMed: 8630490]
- Chalupa, LM.; Williams, RW. *Eye, Retina, and Visual System of the Mouse, Chapter IV, Development of the Mouse Eye.* The MIT Press; Cambridge, MA: 2008.
- Dyer MA. Regulation of proliferation, cell fate specification and differentiation by the homeodomain proteins, Prox1, Six3, and Chx10 in the developing retina. *Cell Cycle.* 2003; 2:350–357. [PubMed: 12851489]
- Fu X, Kiyama T, Li R, Russell M, Klein WH, Mu X. Epitope-tagging Math5 and Pou4f2: new tools to study retinal ganglion cell development in the mouse. *Dev. Dyn.* 2009; 238:2309–2317. [PubMed: 19459208]
- Hatakeyama J, Kageyama R. Retinal cell fate determination and bHLH factors. *Semin. Cell, Dev. Biol.* 2004; 15:83–89. [PubMed: 15036211]
- Hatakeyama J, Tomita K, Inoue T, Kageyama R. Roles of homeobox and bHLH genes in specification of a retinal cell type. *Development.* 2001; 128:1313–1322. [PubMed: 11262232]
- Inoue T, Hojo M, Bessho Y, Tano Y, Lee JE, Kageyama R. Math3 and NeuroD regulate amacrine cell fate specification in the retina. *Development.* 2002; 129:831–842. [PubMed: 11861467]
- Kagalwala MN, Singh SK, Majumder S. Stemness is only a state of the cell. *Cold Spring Harb. Symp. Quant. Biol.* 2008; 73:227–234. [PubMed: 19150961]
- Lamba D, Karl M, Reh T. Neural regeneration and cell replacement: a view from the eye. *Cell Stem Cell.* 2008; 2:538–549. [PubMed: 18522847]
- Le TT, Wroblewski E, Patel S, Riesenberger AN, Brown NL. Math5 is required for both early retinal neuron differentiation and cell cycle progression. *Dev. Biol.* 2006; 295:764–778. [PubMed: 16690048]
- Liang L, Sandell JH. Focus on molecules: homeobox protein Chx10. *Exp. Eye Res.* 2008; 86:541–542. [PubMed: 17582398]
- Lin B, Wang SW, Masland RH. Retinal ganglion cell type, size, and spacing can be specified independent of homotypic dendritic contacts. *Neuron.* 2004; 43:474–485.
- Liu H, Etter P, Hayes S, Jones I, Nelson B, Hartman B, Forrest D, Reh T. NeuroD1 regulates expression of thyroid hormone receptor 2 and cone opsin in the developing mouse retina. *J. Neurosci.* 2008; 28:749–756. [PubMed: 18199774]
- Livesey FJ, Cepko CL. Vertebrate neural cell-fate determination: lessons from the retina. *Nat. Rev. Neurosci.* 2001; 2:109–118.
- Mao CA, Kiyama T, Pan P, Furuta Y, Hadjantonakis AK, Klein WH. Eomesodermin, a target gene of Pou4f2, is required for retinal ganglion cell and optic nerve development in the mouse. *Development.* 2008a; 135:271–280. [PubMed: 18077589]
- Mao CA, Tsai WW, Barton MC, Klein WH. Neuronal transcriptional repressor REST suppresses an Atoh7-independent program for initiating retinal ganglion cell development. *De. Biol.* 2010 (under review).

- Mao CA, Wang SW, Pan P, Klein WH. Rewiring the retinal ganglion cell gene regulatory network: Neurod1 promotes retinal ganglion cell fate in the absence of Math5. *Development*. 2008b; 135:3379–3388. [PubMed: 18787067]
- Marquardt T, Ashery-Paden R, Andrejewski N, Scardigli R, Guillemot F, Gruss P. Pax6 is required for the multipotent state of retinal progenitor cells. *Cell*. 2001; 105:43–55. [PubMed: 11301001]
- Marquardt T, Gruss P. Generating neuronal diversity in the retina: one for nearly all. *Trends Neurosci*. 2002; 25:32–38. [PubMed: 11801336]
- Moshiri A, Gonzalez E, Tagawa K, Wang M, Frishman LJ, Wang SW. Near complete loss of retinal ganglion cells in the math5/brn3b double knockout elicits severe reductions of other cell types during retinal development. *Dev. Biol*. 2008; 316:214–227. [PubMed: 18321480]
- Mu X, Fu X, Beremand PD, Thomas TL, Klein WH. Gene regulation logic in retinal ganglion cell development: Isl1 defines a critical branch distinct from but overlapping with Pou4f2. *Proc. Natl. Acad. Sci. U. S. A.* 2008; 105:6942–6947. [PubMed: 18460603]
- Mu X, Fu X, Sun H, Beremand PD, Thomas TL, Klein WH. A gene network downstream of transcription factor Math5 regulates retinal progenitor cell competence and ganglion cell fate. *Dev. Biol*. 2005; 280:467–481. [PubMed: 15882586]
- Mu X, Klein WH. A gene regulatory hierarchy for retinal ganglion cell specification and differentiation. *Semin. Cell Dev. Biol*. 2004; 15:115–123. [PubMed: 15036214]
- Mu, X.; Klein, WH. Gene regulatory networks and retinal ganglion cell Development. In: Chalupa, LM.; Williams, RW., editors. *Eye, Retina, and Visual System of the Mouse*. The MIT Press; Cambridge, MA: 2008. p. 321-332.
- Ohsawa R, Kageyama R. Regulation of retinal cell fate specification by multiple transcription factors. *Brain Res*. 2008; 4:1192, 90–98.
- Oran-Karni V, Fahy C, Elgart M, Remizova L, Yaron D, Xie Q, Cveki A, Ashery-Paden R. Dual requirement for Pax6 in retinal progenitor cell. *Development*. 2008; 135:4037–4047. [PubMed: 19004853]
- Pan L, Deng M, Xie X, Gan L. ISL1 and BRN3B co-regulate the differentiation of murine retinal ganglion cells. *Development*. 2008; 135:1981–1990. [PubMed: 18434421]
- Pennesi ME, Cho JH, Wu SH, Zhang J, Wu SM, Tsai MJ. BETA2/NeuroD1 null mice: a new model for transcription factor-dependent photoreceptor degeneration. *J. Neurosci*. 2003; 23:453–461. [PubMed: 12533605]
- Riesenberg AN, Lee TT, Willardsen MI, Blackburn DC, Vetter ML, Brown NL. Pax6 regulation of Math5 during mouse retinal neurogenesis. *Genesis*. 2009a; 47:175–187. [PubMed: 19208436]
- Riesenberg AN, Liu Z, Kopan R, Brown NL. Rbpj cell autonomous regulation of retinal ganglion cell and cone photoreceptor fates in the mouse retina. *J. Neurosci*. 2009b; 29:12865–12877. [PubMed: 19828801]
- Vetter ML, Brown NL. The role of basic helix-loop-helix genes in vertebrate retinogenesis. *Semin. Cell Dev. Biol*. 2001; 12:491–498. [PubMed: 11735385]
- Willardsen MI, Suli A, Pan Y, Marsh-Armstrong N, Chien CB, El-Hodiri H, Brown NL, Moore KB, Vetter ML. Temporal regulation of Ath5 gene expression during eye development. *Dev. Biol*. 2009; 326:471–481. [PubMed: 19059393]
- Wang SW, Kim BS, Ding K, Wang H, Sun D, Johnson RL, Klein WH, Gan L. Requirement for math5 in the development of retinal ganglion cells. *Genes Dev*. 2001; 15:24–29. [PubMed: 11156601]
- Yang Z, Ding K, Pan L, Deng M, Gan L. Math5 determines the competence state of retinal ganglion cell progenitors. *Dev. Biol*. 2003; 264:240–254. [PubMed: 14623245]

Research Highlights

- Spatiotemporal expression pattern of the bHLH gene *Atoh7* in retinal development
- *Atoh7* is expressed in both postmitotic and proliferating retinal progenitor cells
- *Pax6* and *Atoh7* are co-expressed in RPCs during early stages of retinal development
- Distinct subpopulations of RPCs express *Atoh7*, *Neurod1*, or both *Atoh7-Neurod1*
- *Atoh7-Neurod1* double mutant retinas reveal a role for *Neurod1* in RGC specification

**Figure 1.**

Expression of HA and lacZ in *Atoh7^{HA/lacZ}* retinas. (A) *Atoh7^{HA/LacZ}* retinas at E14.5 were immunohistochemically labeled with anti-HA antibody (brown) and histological stained for X-gal (blue). The ganglion cell layer is at the bottom on the image. (B) Histogram showing the temporal expression pattern of *Atoh7-HA* in the neuroblast layer of developing retinas. *Atoh7*-expressing cells from E12.5 to E19.5 were detected by immunolabeling retinas with anti-HA antibody. To identify cells, their nuclei were stained with propidium iodide (PI). The number of HA-positive cells and nuclei in the neuroblast layer were quantified as described in the Methods section. The HA-positive cells are calculated as a fraction of total cells in the neuroblast layer (n=3).

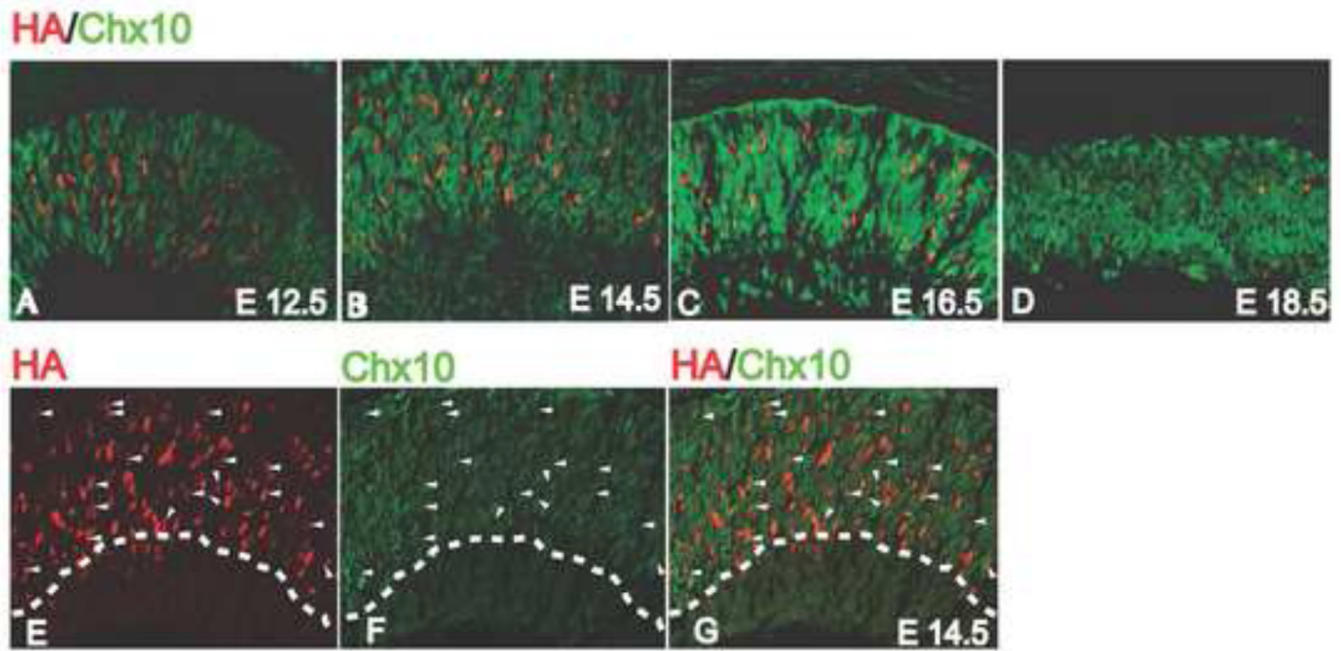


Figure 2. Co-expression of HA and Chx10 in developing retinas. (A–D) Retinas co-labeled with anti-HA (red) and anti-Chx10 (green) antibodies at the indicated developmental stages. (E–G) Double labeling of Chx10 and HA in E14.5 retina. Stained retinae are represented as HA-staining (E), Chx10 staining (F) and merge (G). Cells co-labeled with HA and Chx10 antibodies are indicated by an arrow head.

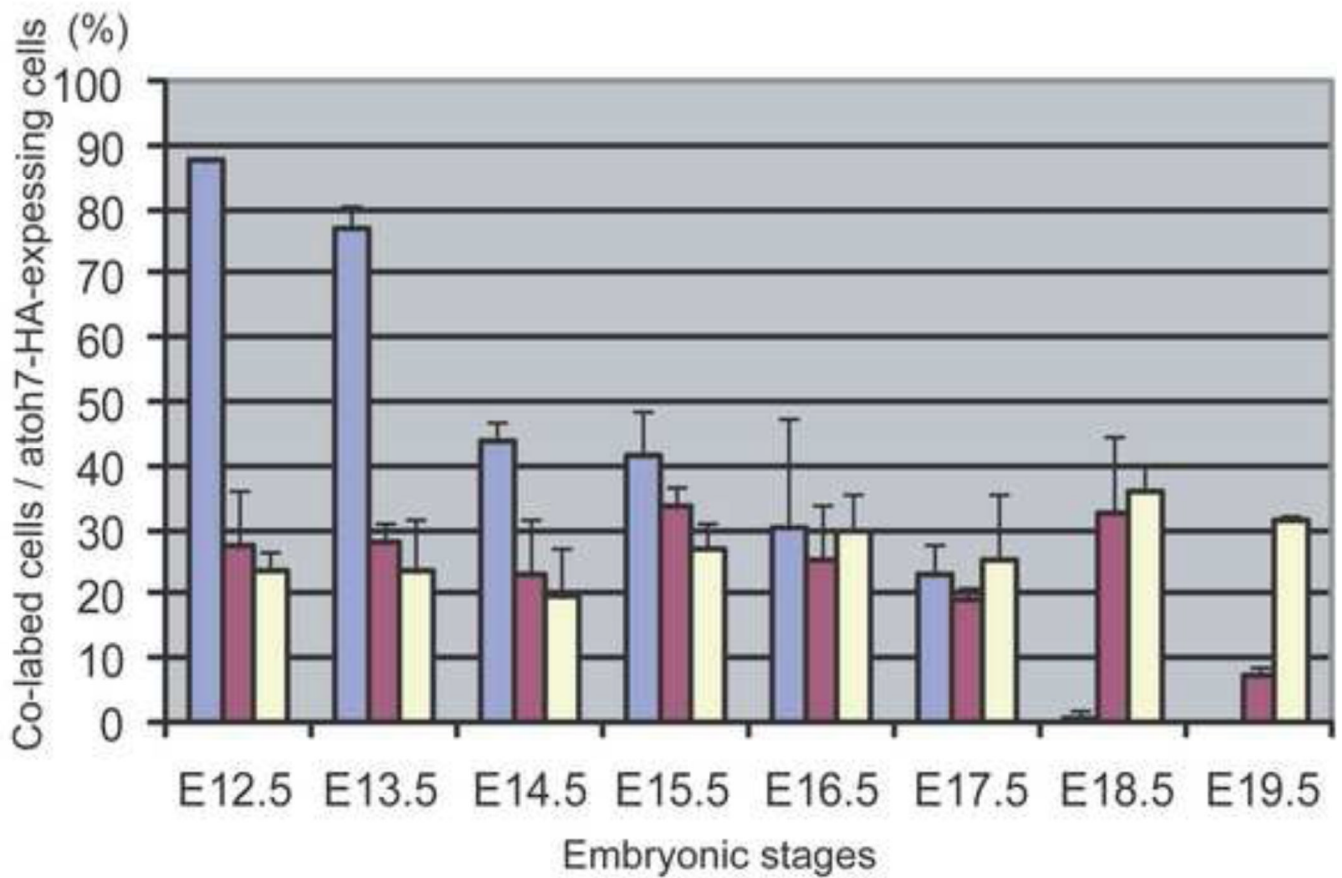


Figure 3.

Histogram showing the fraction of *Atoh7*-expressing RPCs in the neuroblast layer of the developing retinas that are co-expressing *Pax6* (blue-gray), *Chx10* (red) or *Neurod1* at the indicated developmental times. Anti-HA, anti-Pax6, and anti-Neurod1 antibodies were used to label the retinas (n=3) and the fraction of cells expressing the indicated transcription factor was determined as described in the Methods section.

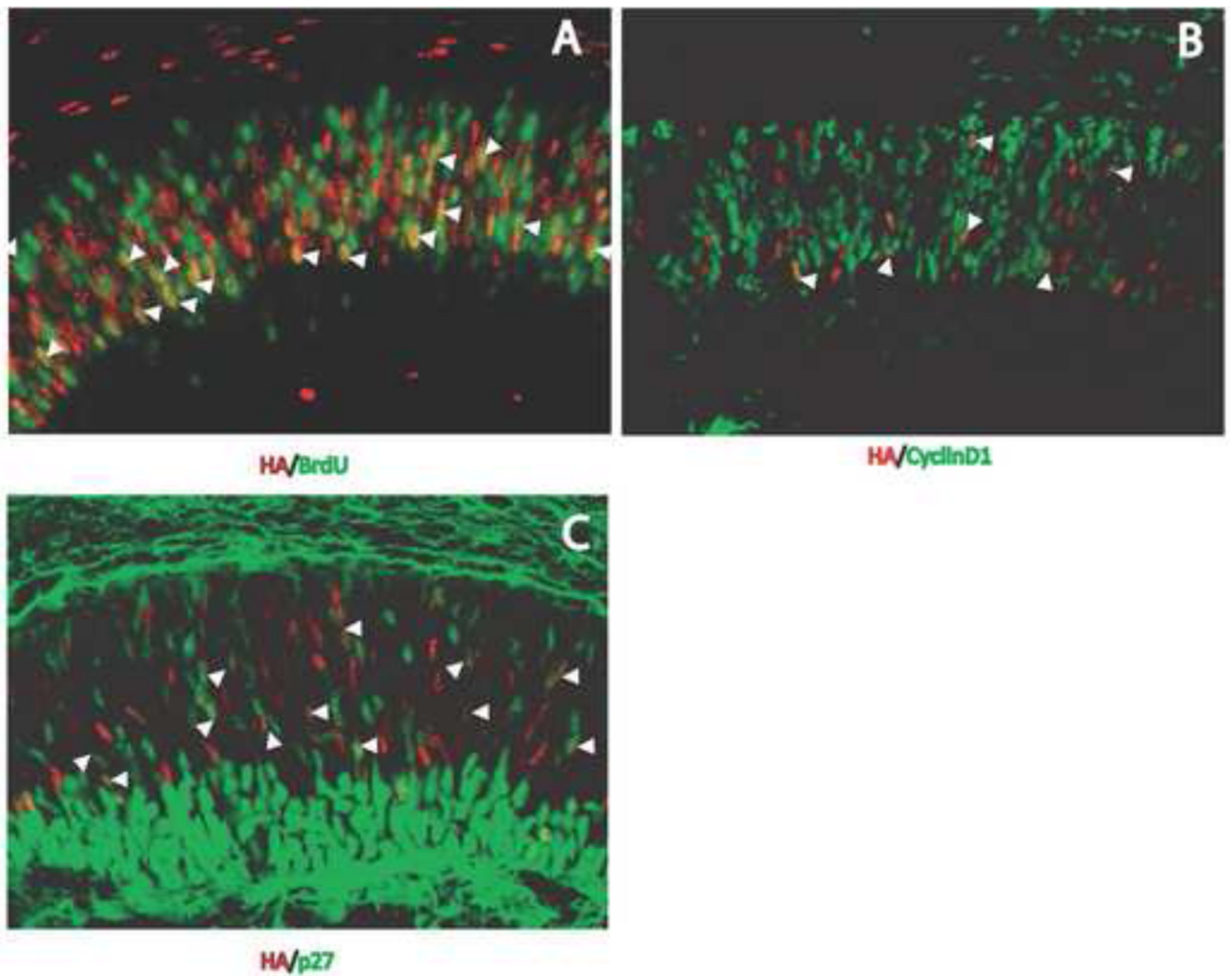


Figure 4. Co-expression of *Atoh7-HA* with cell cycle markers. Retinas at E14.5 were immunolabeled with anti-HA antibody (red) and antibodies against BrdU (A), cyclinD1 (B), or p27 (C) (green). Cells co-labeled with anti-HA and anti-BrdU, anti-CyclinD1 or anti-p27 antibodies are indicated by the arrowheads.

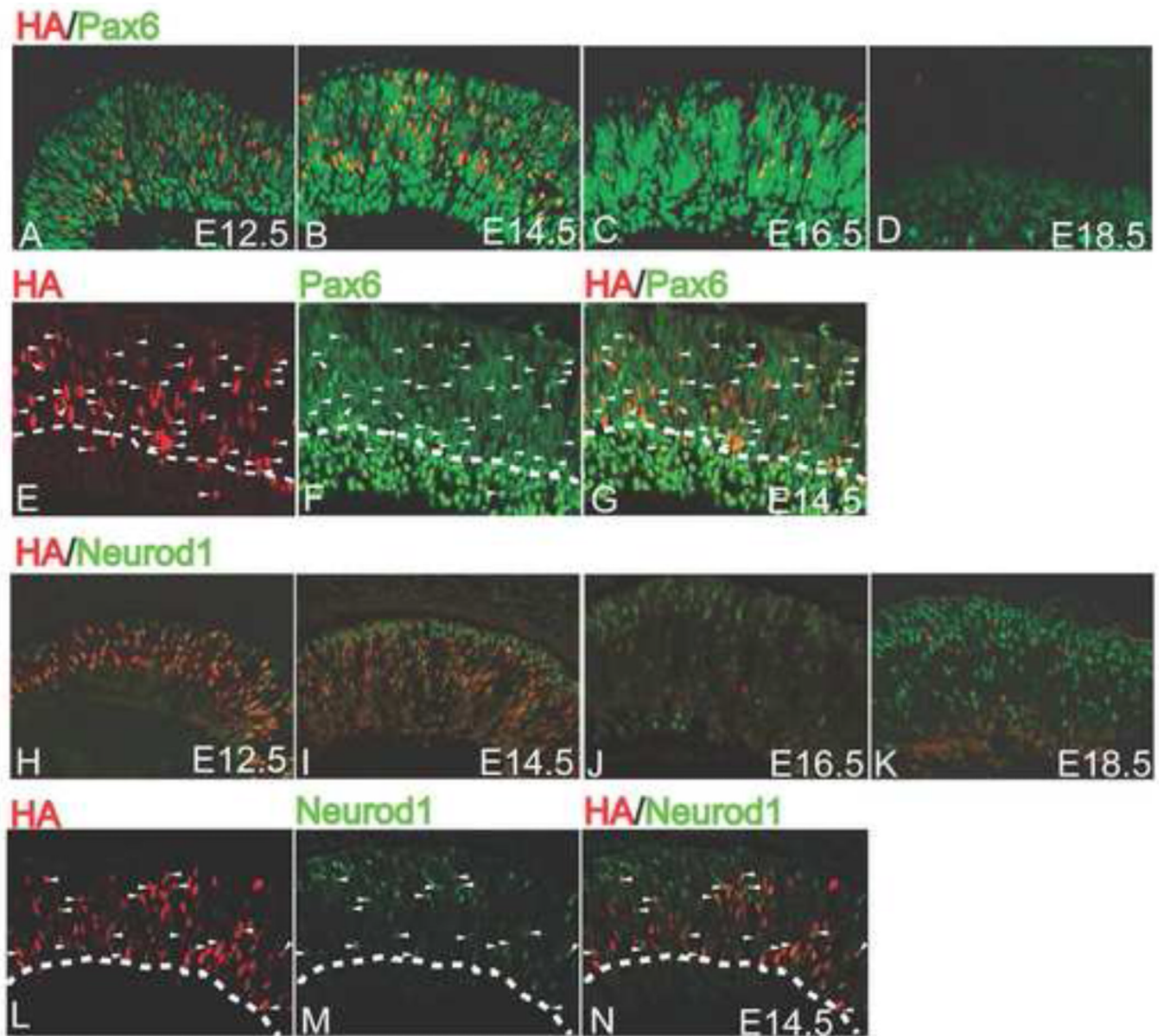


Figure 5. Co-expression of *Atoh7* with *Pax6* (A–D) or *Neurod1* (E–H). Retinas at the indicated developmental times were immunolabeled with anti-HA (red) and anti-Pax6 or anti-Neurod1 (green) antibodies.

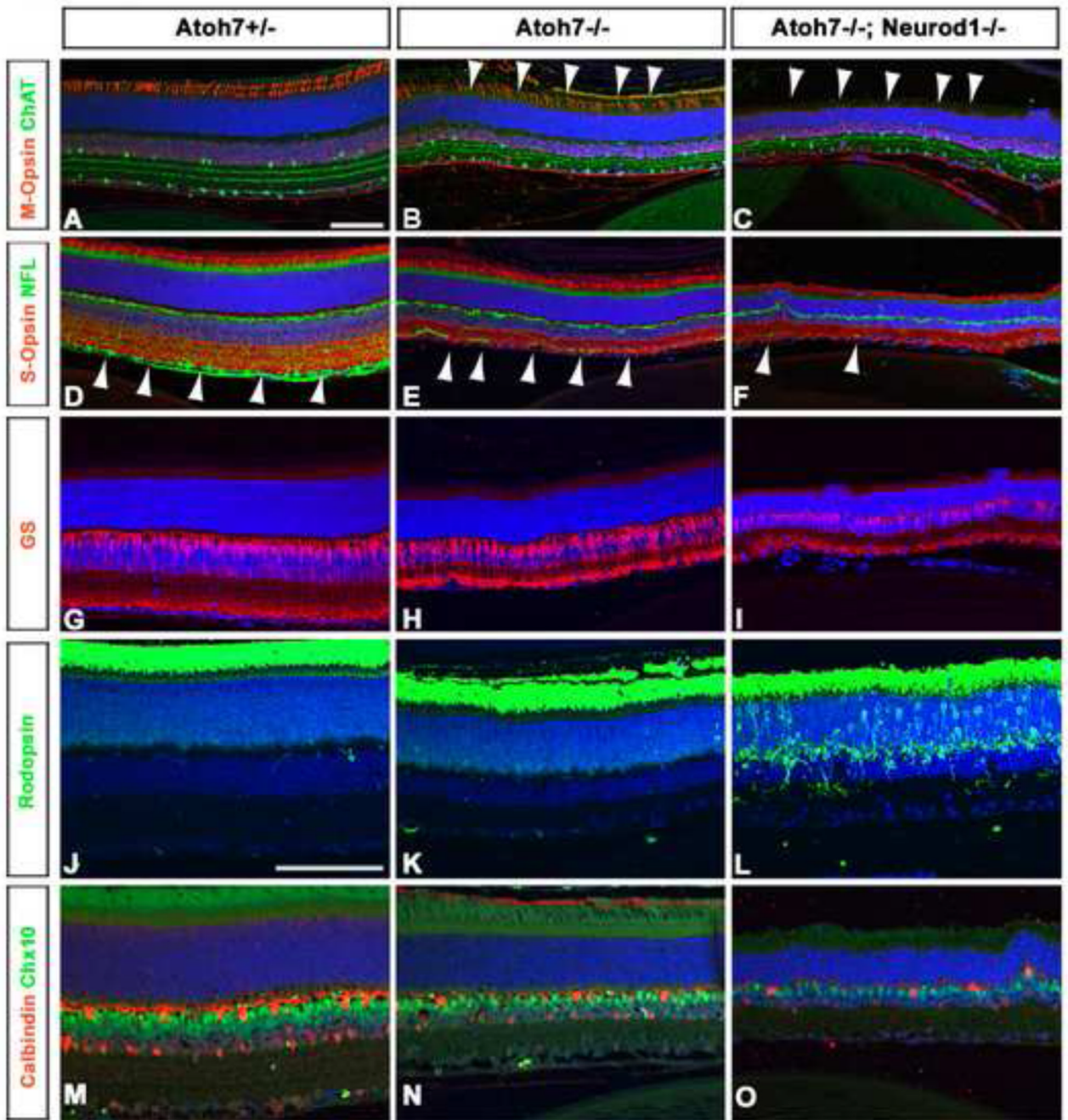


Figure 6.

Retinal cell types in *Atoh7*^{+/-} (left panels), *Atoh7*^{-/-} (middle panels) and *Atoh7-Neurod1* double mutant (right panels) retinas at P35. Cell types were identified by immunohistochemical labelling with the indicated antibody: anti-Chat, amacrine cells (A–C, green), anti-M-opsin, M-cone photoreceptors (A–C, red), anti-NFL RGCs (D–F, green), anti-S-opsin, S-cone photoreceptors (D–F, red), anti-glutamine synthase (GS), Müller glial cells (G–I, red), anti-rhodopsin rod photoreceptors (J–L, green), Chx10, bipolar cells (M–O, green), and anti-calbindin, horizontal cells (M–O, red). Scale bar in panels A, J, 50 μ m.

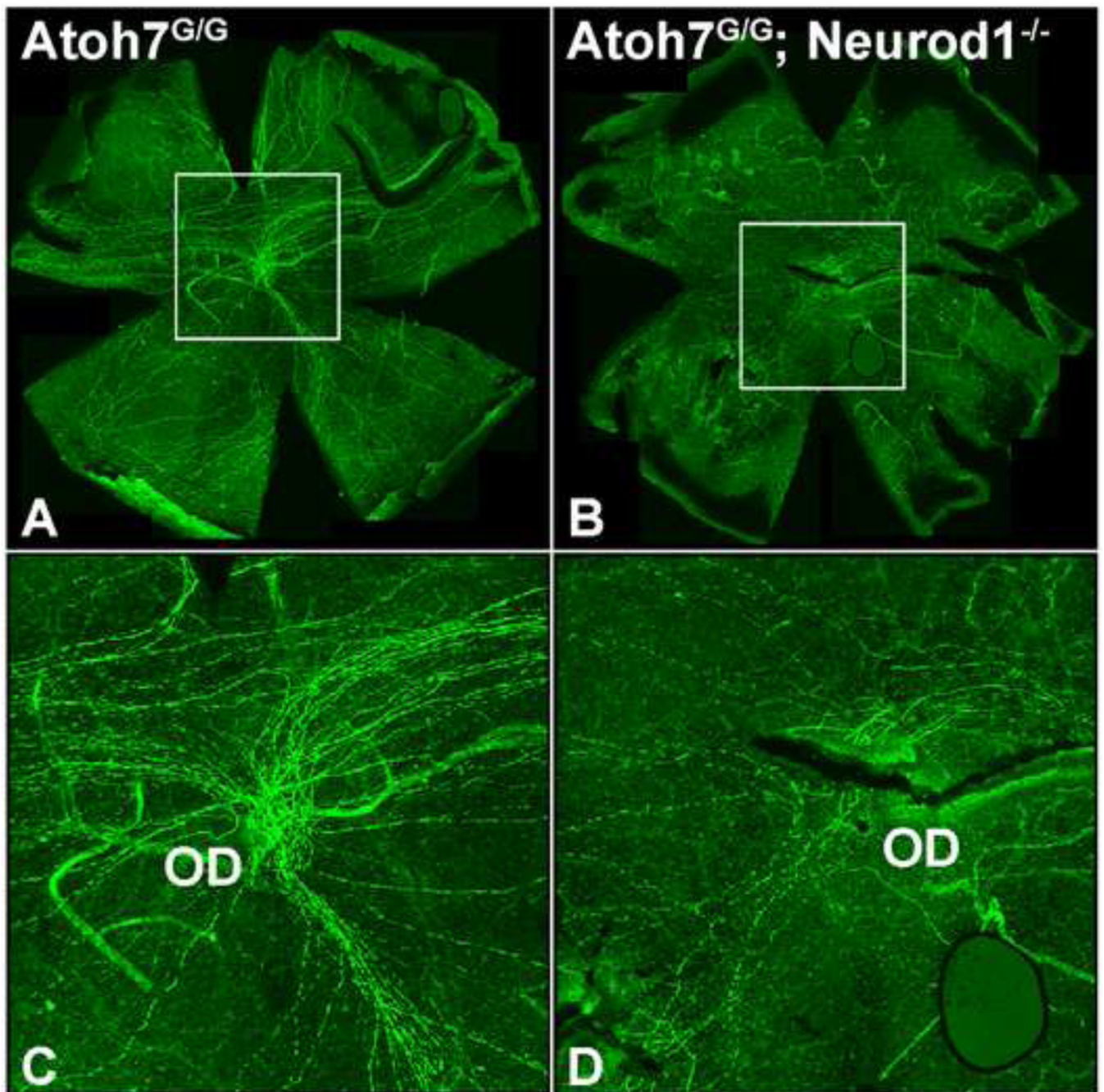


Figure 7. *Atoh7-Neurod1* double-mutant retinas contain fewer RGC axon fibers than do *Atoh7* mutant retinas. (A, B) Immunolabeling of flat-mounted retinas from P30 mice with anti-NFL antibody to reveal RGC axons. Genotypes are indicated on the upper left of each panel. (C, D) Enlarged images of boxed areas in panels A and B highlight the reduced number of axon fibers in *Atoh7-Neurod1* double mutants. OD, optic disk.

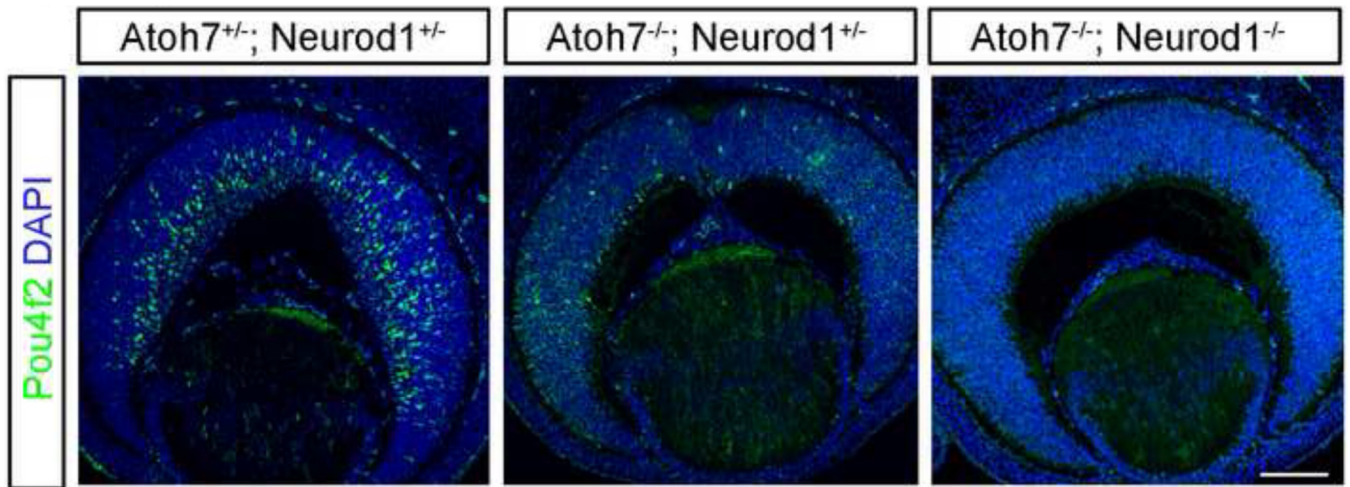


Figure 8. *Pou4f2* expression in E13.5 *Atoh7* and *Neurod1* mutant retinas. (A) *Atoh7*^{+/+}; *Neurod1*^{+/+}, (B) *Atoh7*^{-/-}; *Neurod1*^{+/+}, and (C) *Atoh7*^{-/-}; *Neurod1*^{-/-} retinas. Scale bar in C, 100 μm.

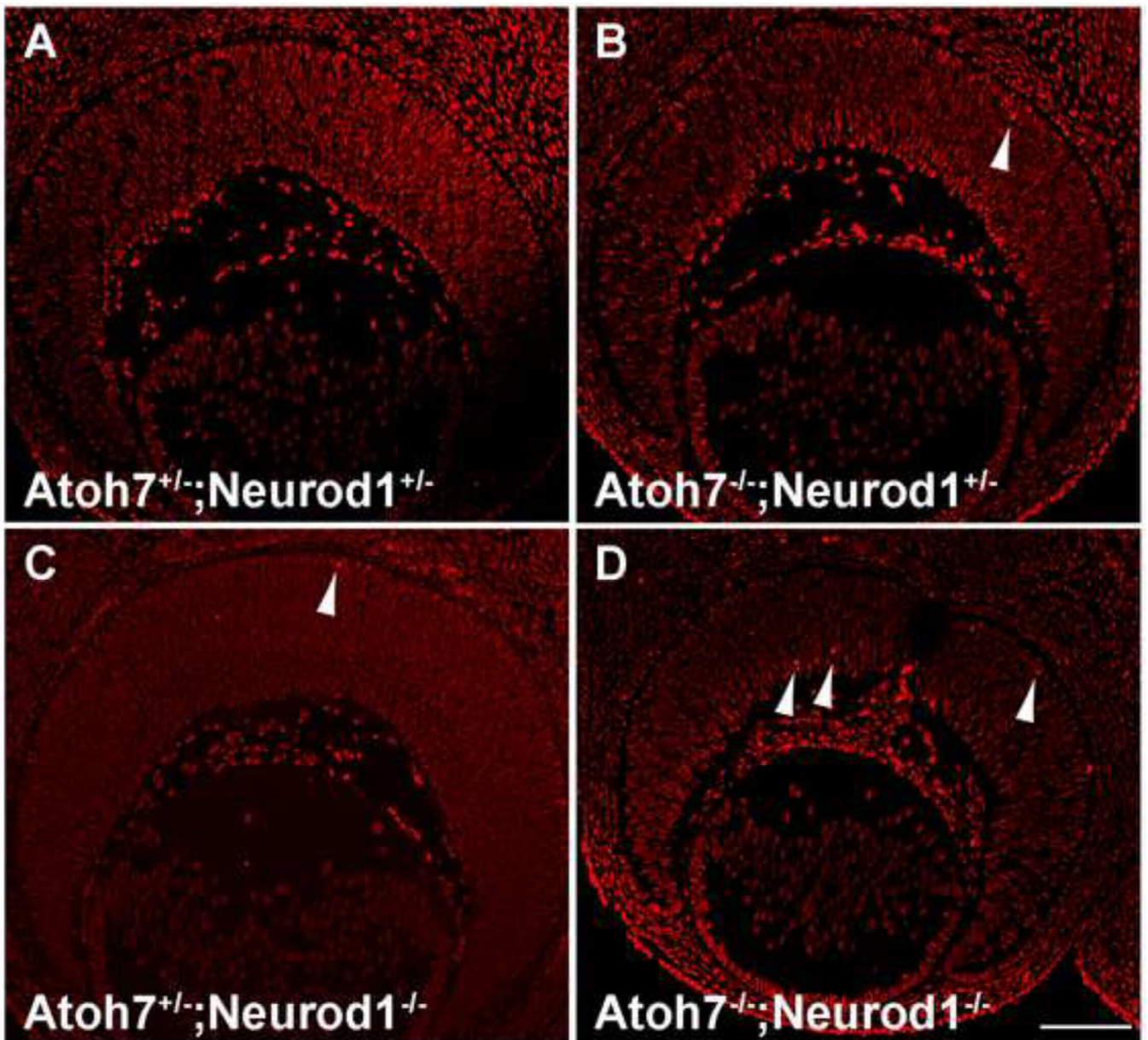


Figure 9. Apoptosis analysis in E14.5 *Atoh7* and *Neurod1* mutant retinas. (A) *Atoh7*^{+/-}; *Neurod1*^{+/-}, (B) *Atoh7*^{-/-}; *Neurod1*^{+/-}, (C) *Atoh7*^{+/-}; *Neurod1*^{-/-}, and (D) *Atoh7*^{-/-}; *Neurod1*^{-/-} retinas. Note that a slight increase of cell death is always found in *Atoh7*^{-/-}; *Neurod1*^{-/-} retinas than in control retinas. Arrowheads indicate dying cells. Scale bar in D, 100 μ m.